Scientific Research Publishing

Open Journal of Antennas and Propagation, 2025, 13(2), 35-48
https://www.scirp.org/journal/ojapr
ISSN Online: 2329-8413
ISSN Print: 2329-8421

A Study on the Influence of Solar Flares on High Frequency Radio Propagation

Khoder Khaled[1], Ahmad El Sayed Ahmad[1], Pascal Pagani[2], Rolland Fleury[2]

[1]Capgemini Engineering, Toulouse, France
[2]Lab-STICC, UMR 6285, Institut Mines-Télécom Atlantique, Brest, France
Email: khaled.khoder@capgemini.com

How to cite this paper: Khaled, K., El Sayed Ahmad, A., Pagani, P. and Fleury, R. (2025) A Study on the Influence of Solar Flares on High Frequency Radio Propagation. *Open Journal of Antennas and Propagation*, **13**, 35-48.
https://doi.org/10.4236/ojapr.2025.132003

Received: June 1, 2025
Accepted: June 27, 2025
Published: June 30, 2025

Abstract

On 25 October 2013, the Sun emitted two significant solar flares. The first solar flare, classified X1.7, peaked at 08:01 UT. The second one, X2.1, peaked at 15:03 UT and was accompanied by solar radio emission. In this work, we study the ionospheric response to the two X-class solar flares and their impact on high-frequency (HF) propagation. For this aim, opportunistic HF signals are used; these signals correspond to any HF communication signal using the ionospheric channel as a transmission medium. First, an identification procedure of opportunistic HF radio waves is presented using measurements performed in the cities of Toulon, France (43.11˚N; 5.93˚E) and Brest, France (48.40˚N; 4.48˚W). Among several identified HF transmitters, those which are in operation during the two solar flares are selected. In the second part, we present some information confirming the detection of two solar flares on 25 October and study their effects on HF signals received in France.

Keywords

Solar Flare, X-ray Flux, Ionosphere, HF Propagation, Sudden Ionospheric Disturbance, Broadcast Transmitters

1. Introduction

The ionosphere is described as the Earth's atmospheric layer, which is ionized by solar and cosmic radiation [1] [2]. It refers to upper atmospheric regions (90 to 1000 km). This area is heavily ionized, meaning it has a high free electrons density (negative charges) and positively charged ions. It has functional significance, because it allows HF radio propagation to distant places on earth [3]-[5]. This specific behavior depends on both the frequency of the radio signal as well as the characteristics of the ionosphere region involved.

In the ionosphere, however, solar radiation (mainly ultraviolet) is so intense that when it hits gas molecules, it partitions them (it is said to ionize them) and an electron is thus released. This results a positive ion (molecule or atom missing an electron) and a free electron. Although it is the ions that have given this region its name, it is mainly electrons that affect radio waves. The number of electrons begins to grow at an altitude of about 30 km but the density of electrons is not sufficient to affect radio waves up to about 60 km. The electron concentration occurs in vertically stratified regions, also called ionospheric layers. Three main layers are identified within the ionosphere: The D layer, the E layer, and the F layer. There is also a C-layer, but its ionization level is so low that it has no detectable effect on radio waves [1].

The D-layer is the closest to the Earth's surface. Its altitude is between 50 km and 90 km. Because of the high density of gases, the recombination process is very active and the electron density is very low [6]. This layer is mostly present during the day, but cosmic radiation maintains a residual ionization during the night. It does not reflect HF waves but absorbs them, mainly at low frequencies. As a result, absorption is lower at night, and wave propagation is therefore better at night. The E layer is located at higher altitudes, between 90 km and 120 km. It mainly reflects waves of relatively low frequencies, less than about 10 MHz, and partially absorbs higher frequencies [7]. The maximum density in the E layer occurs near 100 km**,** although this height varies with local time. During the nighttime, the ionization in the E region approaches small residual levels [8].

The F layer extends from 120 km to 400 km in altitude. It is the densest upper layer and is open to the outside, *i.e.* towards the magnetosphere. It will therefore be the preferred layer for establishing HF links and will be sensitive to variations in density and therefore to solar activity. During the day, it can be divided into two layers, called F1 and F2 [6]. Consequently, the F layer has diurnal variations (day/night), seasonal changes (summer/winter) and is strongly disturbed by solar activity. The separation between E and F is related to the difference of neutral constituents (nitrogen, molecular and atomic oxygen) as well as the concentration.

A wave emitted at a fixed elevation angle penetrates the ionospheric layers the higher its frequency. Above a certain frequency, the wave passes through the ionosphere without being refracted towards the ground. There is therefore an upper frequency limit, imposed by ionospheric refraction, above which binding is no longer possible. This limit is called MUF (Maximum Usable Frequency). A lower limit called LUF (Lowest Usable Frequency) is imposed by the need for sufficient field strength at reception. A link using the ionospheric channel can therefore only be operated in a frequency band between the LUF and the MUF.

However, the ionosphere exhibits diurnal changes (day/night), seasonal changes (summer/winter) and is strongly affected by solar activity (11-year cycle, solar flares...).

In this paper, the effect of Sudden Ionospheric Disturbance (SID) on HF waves

is studied. An SID consists of an increase in the electron density of the D-layer following a solar flare in which the part of the Earth illuminated by the sun is subjected to a bombardment of X-rays and UV radiation [9]-[13]. This radiation penetrates to the D-layer and increases the ionization process and electron density. This creates severe temporary disruptions in the ionosphere, and increases the absorption of radio waves mainly in the HF band (3 MHz - 30 MHz), narrowing the range of possible frequencies for a given link [14].

To study the effect of solar flares on HF waves propagation, the idea here is to use opportunistic HF signals. These signals correspond to any HF communication signal using the ionospheric channel as a transmission medium. The idea is to capture these signals passively and extract information on the variation of the ionosphere during solar flares. The advantage of using these signals is that they are powerful and have known characteristics.

In [15], we have proposed a procedure of identification of opportunistic HF radio waves. In a first section, we will describe briefly this procedure and will give some examples of identified transmitters around the word. In a next section, which is the purpose of this paper, we will concentrate on HF transmitters operating during the occurrence of solar flares to study their effect.

2. HF Transmitters Identification

2.1. Available Data

The data used in this research covers 7 years of field measurements performed in the city of Toulon, France (43.11˚N; 5.93˚E) and two-month measurements in the city of Brest, France (48.40˚N; 4.48˚W). Measurements performed in Toulon correspond to one measuring point every two hours in the 5800 - 17,900 kHz range, with a frequency step of 0.1 kHz. Such data allow us to classify frequencies used by radio transmitters, with high measured field values. Measurements in Brest are performed with one measurement point every 15 minutes. These measurements should provide us with more precise information about the transmitters, such as the start and stop time of the emission during the day. We referred to the BRIFIC database [16] maintained by the ITU (International Telecom Union) for information on the operating transmitters and their characteristics (power, location, operating hours, emission zone...). Eventually, a test can be made after identification of a transmitter by listening to the transmitted audio signal using dedicated web resources [17]. This allows us to validate the radio broadcast transmitter,by verifying the operation hours or the program language.

2.2. Validation Procedure

Using measurements performed in Toulon, our research is focused on the identification of frequencies with high-received electric fields. At these frequencies and based on the measurements made in Brest, the start and end time of the transmission is specified. By referring to the BRIFIC database, we look for transmitters that transmit at the specific frequency and identify the transmitter according to the

transmission times. The flowchart of this procedure is shown in Figure 1.

The data performed in Toulon were plotted as frequency spectra, each peak corresponds to a transmitter; the field strength depends on the transmitter power and the regions targeted by the transmitter. The measurements performed in Brest (one measurement point every quarter of an hour) will help us to check the start and end time of transmission for a given transmitter and at a given frequency. Let's take the example of the transmitter transmitting at the frequency 13,635 kHz. The relative measured field at the receiver of Brest is given in Figure 2. In this figure, each point represents a one-day measurement for a specific time.

Several transmitters transmit at the frequency 13,635 kHz. The first and most interesting one transmits between 6:00 and 13:00 UT, *i.e.*, 7 hours of continuous transmission. The received electric field is the strongest among the other transmitters. Other transmitters exist (around 15 h and 18 h) but there are link failures. This may be due to the ionosphere or to a cut in the transmitter. The next step is to check in the BRIFIC database, which transmitters are transmitting on this frequency and what time slots of the transmission are. For each transmitter, the database contains the characteristics of the transmission such as power, transmitter location, CIRAF zones (areas to which the transmitter plans to transmit) and antenna type. According to BRIFIC database, the transmitter shown in Figure 2 is called EMR (39.29˚N; 32.51˚E) located in Emirler, Turkey. This transmitter has a high output power [18] (500 kW) and emits during a continuous period of five and seven hours (06:00 to 13:00 UT) to the CIRAF zone number 27 (Northwestern Europe). It transmits every day of the week at 13,635 kHz.

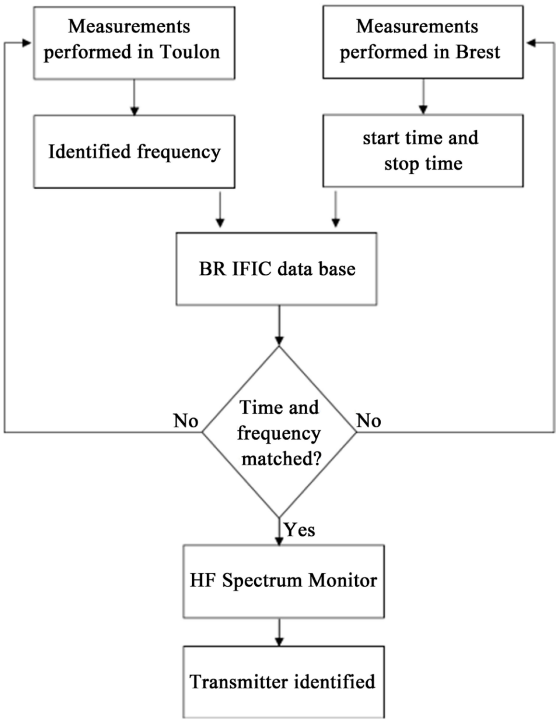

Figure 1. Transmitter identification flowchart.

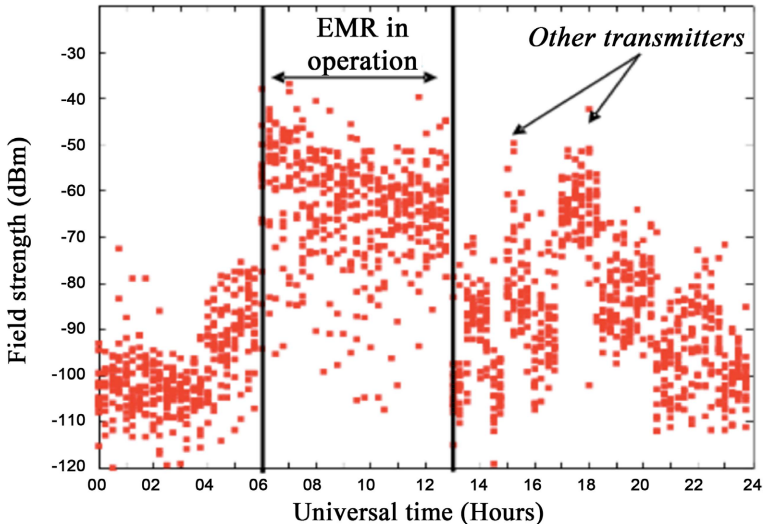

Figure 2. Relative measured field at 13,635 KHz in Brest city.

In order to ensure the identity of this broadcast transmitter, we have listened to this transmitter on the "HF Spectrum Monitor" website. On this site, for a given frequency, we can view the received field strength and listen to the transmitter in real time.

Using the identification procedure, several transmitters were identified in the proposed bands. Transmitters of interest are then selected according to criteria such as the continuity of the transmission on a given band (minimizing frequency sharing), the position of the transmitter, knowledge of the transmitter's characteristics (power, type of antenna, etc.) and most importantly, selected transmitters must be in operation during the occurrence of solar flares.

In the following section, we present some information confirming the detection of two solar flares on 25 October 2013. The influence of these solar flares on HF transmitters will be studied using measurements made in Brest.

3. Effect of Solare Flares on HF Radio Propagation

A Sudden Ionospheric Disturbance is an increase in the electron density of the D-layer following a solar flare [19]-[21]. The part of the Earth illuminated by the sun is then subjected to a bombardment of X-rays and UV radiation [22]-[24]. This radiation penetrates as far as the D-layer and increases the ionization process and electron density [25]-[27]. This increases the absorption of radio waves mainly in the HF band (3 MHz - 30 MHz), narrowing the range of possible frequencies for a given link [28]-[30]. For any given link, SID results in an increase in the LUF since it is the lower frequencies that are affected by the additional absorption phenomenon. In the case of very strong solar flares, the LUF can become higher than the MUF and, in this case, no frequency is passing: we are in the case of a total blackout [31].

Solar flares are a sudden release of energy from the surface of the sun for a few minutes to tens of minutes, in the form of electromagnetic waves over a wide

spectrum (from radio waves to gamma rays to X-rays) and particles of high-energy materials. During a solar flare, the sudden release of energy results in an increase in temperature and acceleration of electrons and protons in the flare zone. The collisions of the high-energy electrons with the atoms of the chromosphere and the corona are the source of the high-energy radiation emissions: EUV and X-rays. X-ray bursts are a signature of the solar flare intensity. They are classified into 4 categories according to their intensity observed on board space satellites in the 1 to 8 Angstrom band: B ($<10^{-6}$), C ($<10^{-5}$), M ($<10^{-4}$) and X ($<10^{-3}$ Watts/m^{-2}) [31].

3.1. Detection of Two Solar Flares during the Day of 25 October 2013

The number of strong solar flares (>M5.5) is limited although we are in the years of the maximum of the solar cycle 24. We have been fortunate to have 2 class X events, associated with daylight hours in Europe and during which we have field measurements in Brest city. In the Hα images of the sun's surface, two large sunspot regions and three smaller ones are shown (upper part of **Figure 3**). It is the complex framed structure of the figure, which interests us because during this day, it will be at the origin of the 2 solar eruptions. The two sunspot regions are also well identified by the measurement of the X-radiation emitted by the GOES 15 satellite and are shown on a color scale (lower part of **Figure 3**).

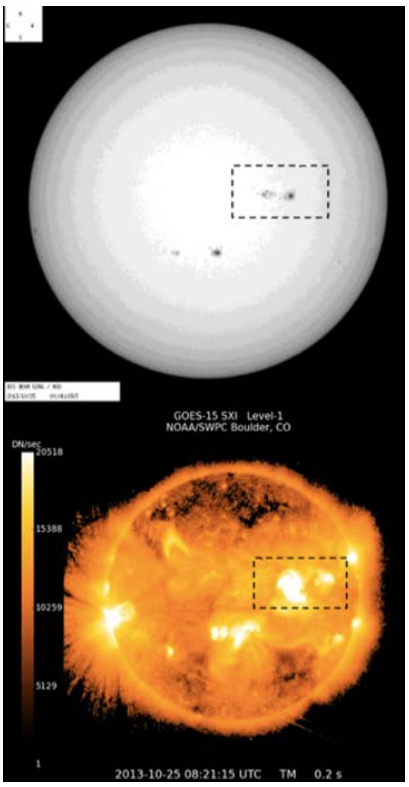

Figure 3. Solar flare on October 25, 2013: (a): Hα image, (b): X-ray radiation.

The SWPC (Space Weather Prediction Center) measurement base [32] is used to visualize the temporal evolution of the intensity of the X-radiation emitted globally by the sun for the period from 24 to 26 October 2013. It is given in **Figure 4**, where the X-ray intensity is shown in red for the 1 to 8 Å band, and in blue for the 0.5 to 4 Å band. Horizontal lines are used to position the measured levels in the different classes identified on the right-hand scale.

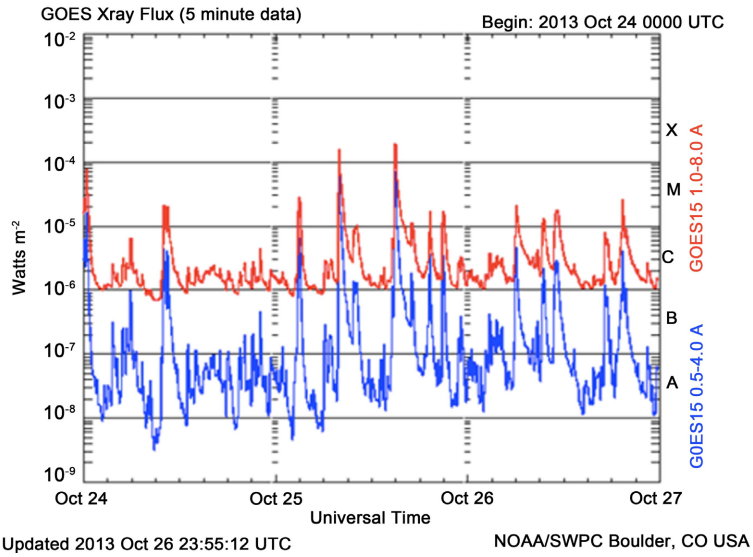

Figure 4. X-ray radiation in watts per meter square from the GOES satellite from 24-27 October.

As sown in **Figure 4**, two powerful X-class solar flares occurred on October 25, 2013. The first flare occurred just before 8:00 UT and the second around 15:00 UT. It is indeed the configuration of a strong level (X1) and a positioning during daylight hours that caught our attention to study the influence of these two solar flares on an HF link. Based on the SWPC online website, the first solar flares start at 7:53 UT, reach its maximum at 8:01 UT and ends at 8:09 UT. The second solar flare starts at 14:51 UT, reach its maximum at 15:03 UT and end at 15:12 UT.

The radiation emitted during a solar flare takes 8 minutes to travel from the sun to Earth and ionize the illuminated D region of the ionosphere. A research is done on ionospheric measurements available on the web during this day and we naturally turned first to the measurements of ionosondes operating vertically. Indeed, the ionosonde is a radar that vertically emits a carrier and measures the arrival time of the reflected echo. The frequency of the carrier sweeps the HF spectrum between 2 - 3 MHz and 30 MHz. As mentioned above, low frequencies are more or less partially absorbed during solar flares and therefore a tracking of the first reflected frequency (called "fmin") should allow quantifying the phenomenon. Ionograms are recorded traces of reflected high-frequency radio pulses generated by ionosondes. Unique relationships exist between the sounding frequency and the ionization densities, which can reflect it. The sounder (ionosonde) sweeps over the noise of commercial radio sources, from lower to higher frequencies, capturing

the return signal that is reflected by the difference ionosphere layers.

Among the ionosonde network operating on 25 October 2013 in Europe, those of Dourbes (Belgium) and Rome (Italy) are selected [33]. With the Dourbes site, sounding is recorded every 5 minutes, which will bring precision in the determination of the period, affected by solar flares. The sounding rate is 15 minutes for all other ionosondes. The values of fmin are determined automatically by the automatic analysis of the profile parameters.

In Figure 5, we gathered the ionogram drawings of Dourbes and indicated the proposed fmin value between 7:55 UT and 8:25 UT, *i.e.*, during the first solar flare.

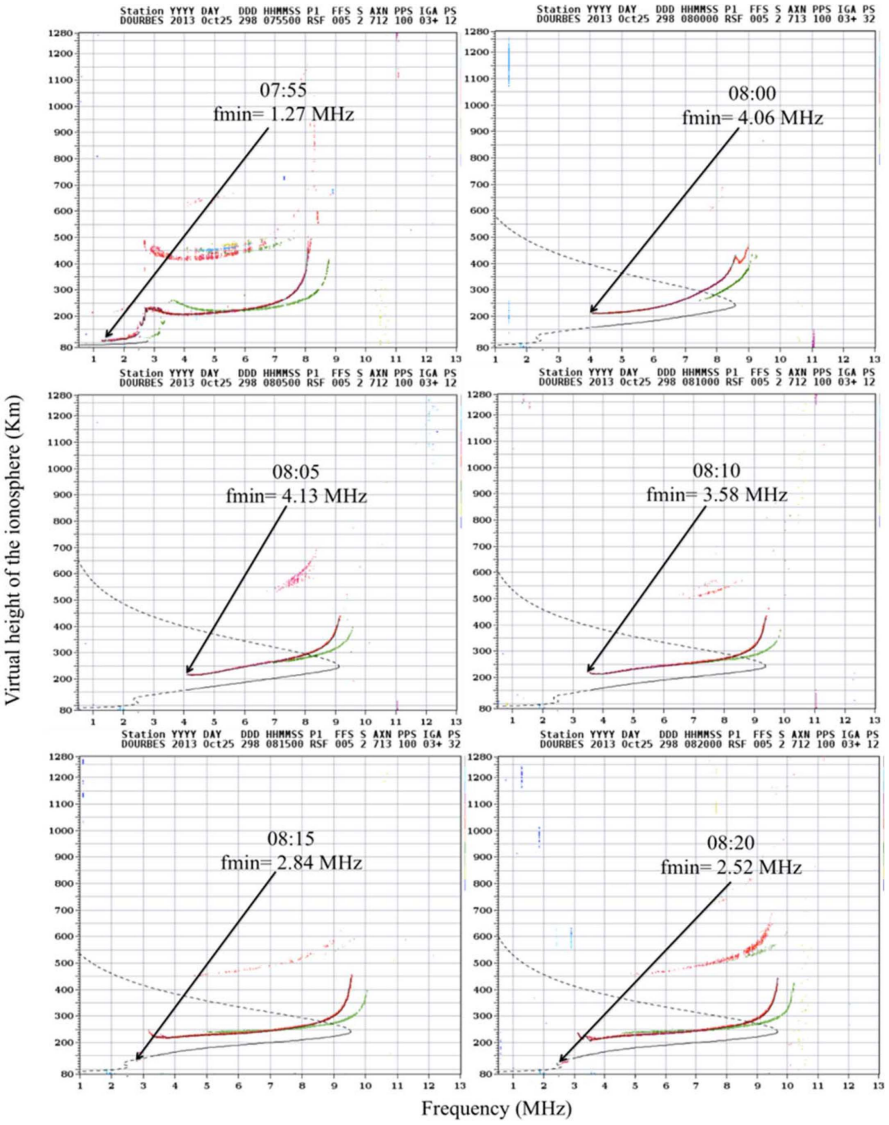

Figure 5. Ionograms obtained from the Dourbes station during the first solar flare.

From Figure 5, it can be seen that the first solar flare was already present at 8:00 UT. In fact, the value of fmin changed from 1.27 MHz (normal value) to 4.06 MHz (abnormal value) between 7:55 UT and 8:00 UT. It can also be indicated that this

solar flare lasted about 20 minutes since the fmin value returned to a normal value (2.52 MHz) at 8:20 UT. This duration is slightly longer than the duration of the flare (16 min) and corresponds to the inertia of the ionosphere.

The ionograms in Rome are registered every 15 minutes; thus, from 7:45 UT to 8:30 UT, four ionograms are obtained and presented in Figure 6.

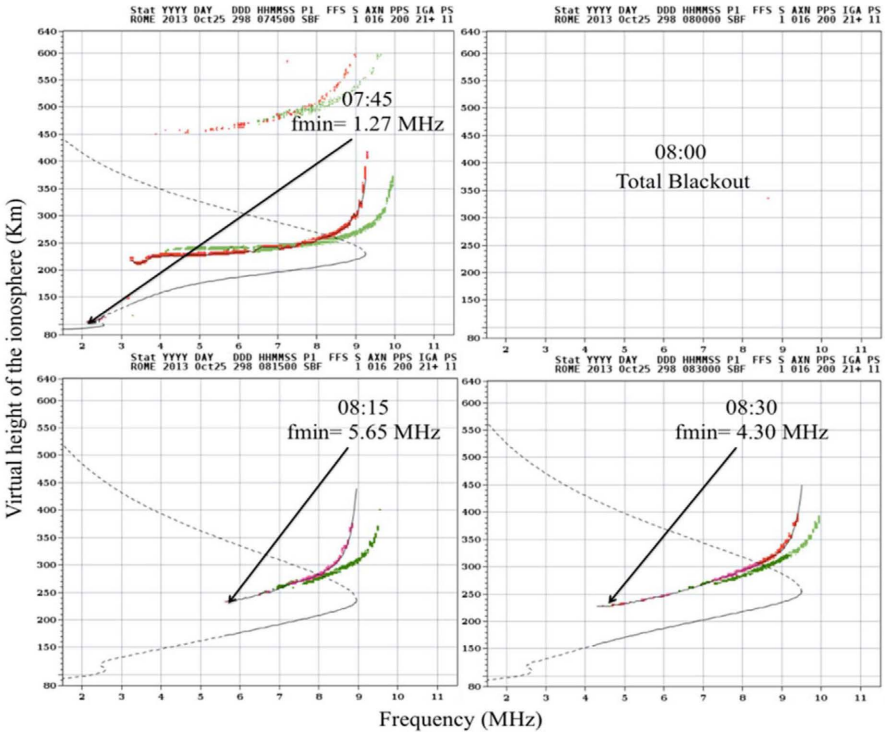

Figure 6. Ionograms obtained from Rome station during the first solar flare.

As can be seen from Figure 6, the solar flare effect measured in Rome is much stronger than that observed at Dourbes since in the figure no return frequency echo is present; *i.e.*, we are in the typical situation of total absorption or 'blackout' at 8:00 UT. The fact of having a total absorption in Rome and not in Dourbes certainly comes from the fact that the latitude of Rome is lower, *i.e.*, closer to the sub-solar point and therefore, the effect would be more important. The duration is also more important. We still measure an fmin value of 4.30 MHz at 8:30 UT.

Similarly, the ionograms of the ionosondes at Dourbes and Rome were studied around 15:00 UT to know the exact time, duration and intensity of the second solar flare. Referring to these ionograms, and analyzing the fmin values, we have concluded that the second solar flare is present at 15:00 UT and the duration is around 10 minutes and therefore slightly shorter than the first solar flare.

The effect of the detected solar flares on HF signals will be studied in the next section using measurements in Brest on the 15 minutes basis.

3.2. Effect of Solar Flares on Received HF Signals

In this section, we will select some of the previously identified transmitters and

study the behavior of their signals during these two solar flares on 25 October 2013. It should be noted that for this study we have one measurement point every 15 minutes in Brest. The influence can only be identified on one or two points since the duration of these solar flares does not exceed 20 minutes according to the conclusion of the fmin measurements. Spectral field strength measurements were performed using calibrated wideband HF receivers connected to omnidirectional antennas oriented vertically to capture skywave propagation. The measurement bandwidth was set to approximately 10 kHz, allowing sufficient resolution for broadcast signal identification.

The first transmitter chosen is the transmitter located in Emirler in Turkey (EMR) identified at the frequency 13,635 kHz. It transmits from 6:00 UT to 13:00 UT to CIRAF zone number 27. We have studied the field strength received at Brest, France for the day of 25 October and for the days of 24 and 26 October (**Figure 7**) to study the possible variability of the signal during solar flares.

It can be seen from **Figure 7** that the level of the field dropped significantly during the solar flare on 25 October. Indeed, the field level decreased by more than 45 dB at 8:00 UT. For the other days, the measured field strength remained at the same level at 8:00 UT. Concerning the duration, the measurements at 8:15, 8:30 and 8:45 UT remain below those obtained on the surrounding days. It is only from 9:00 UT that the normal level is restored. We have a solar flare of about 45 minutes, which is in line with the expected figure given the importance of the solar flare. Concerning the second solar flare of 15:00 UT, no conclusion can be drawn since this transmitter was not using this frequency.

Another transmitter was studied during these three days, the transmitter transmitting from Riyadh (RIY) at the frequency 17,730 kHz (**Figure 8**). It transmits from 6:00 UT to 9:00 UT to CIRAF zones 37 and 38. A 50 dB drop was obtained at 8:00 UT, which is the maximum level of the solar flare.

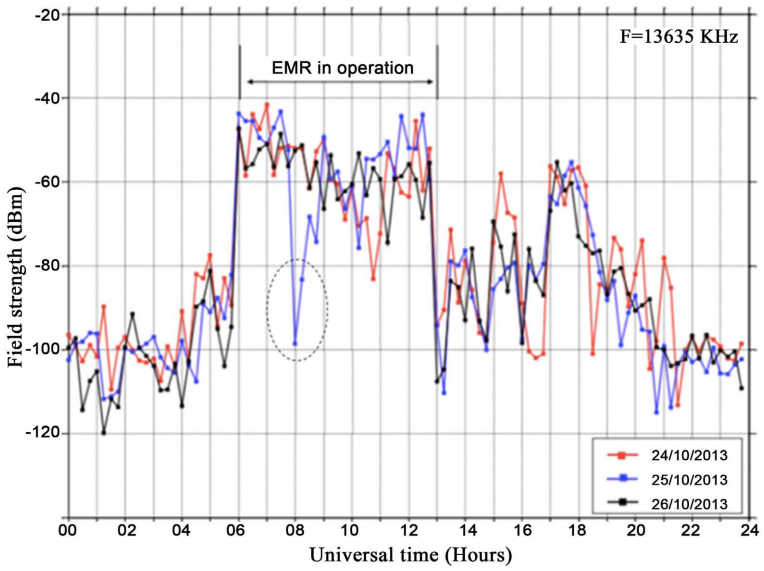

Figure 7. Received field in Brest at 13,635 kHz for the days 24, 25 and 26 October 2013.

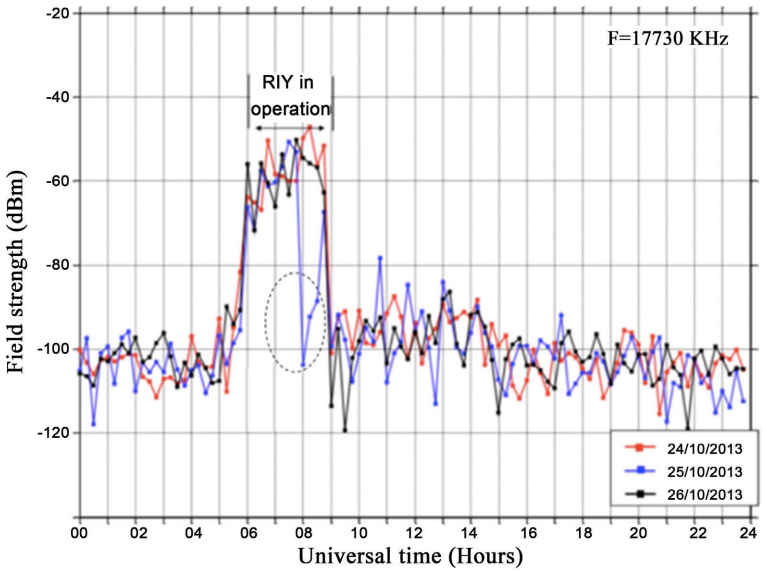

Figure 8. Received field in Brest at 17,730 KHz for the days 24, 25 and 26 October 2013.

4. Conclusions

In this paper, a procedure for identifying radio broadcast transmitters has been developed and tested. We used for this purpose, two databases of measurement performed in the cities of Brest and Toulon, France. This procedure can be generalized and used in the future to build a base of opportunity signals that can be used for other operational applications. The application of the identification procedure to broadcasting transmitters has resulted in the identification of several operable broadcasting transmitters around the word.

The effects of a sudden ionospheric disturbance caused by solar flares on the level of HF signals were studied. In particular, we treated the two very strong solar flares (classified X by the SWPC) that occurred during the day of 25/10/2013 and during which spectral field strength measurements were available over Brest every 15 minutes.

A search has been made on ionospheric measurements available on the web during this day and we first turned naturally to the measurements of ionosondes operating vertically. We chose to use the measurements data of the ionosondes located in Rome and Dourbes. We have shown that the low frequencies are more or less partially absorbed during solar flares and therefore a follow-up of the first reflected frequency (called "fmin") should allow us to quantify the phenomenon.

By superimposing the fmin measurements from the Dourbes and Rome stations with the X-ray radiation measurements on board the GOES-15 satellite, a very good correlation is observed during the phenomenon despite different sampling in the two cases. We have also observed and presented the case where the absorption is total over all the vertical frequencies emitted (blackout). The temporal positioning of the two solar flares was also well identified on the spectral field strength measurements performed in Brest. Attenuations of 40 - 60 dB were measured on

many broadcast transmitters including high frequencies (18 MHz).

These good results obtained from a 15-minute sample show that it is possible to identify the occurrence of solar flares from opportunistic HF signals. To improve performance, it would be preferable to reduce the sampling time to 5 minutes or even 1 minute. In this case, measurements could be limited to a small number of predetermined frequencies. On the other hand, the observed signal spectrum could be complemented by VLF signals, which are less sensitive to time variations and thus allow more reliable detection.

The results presented in this study are based on two solar flare events observed along a single mid-latitude path, specifically over Brest, France. As such, the findings may not fully capture the variability introduced by different seasons, latitudinal positions, or geomagnetic conditions. These factors can significantly influence the depth and duration of HF signal outages, and future studies should aim to incorporate a broader range of geographic and temporal scenarios to validate and extend the applicability of the proposed methodology.

Conflicts of Interest

The authors declare no conflicts of interest regarding the publication of this paper.

References

[1] Zolesi, B. and Cander, L.R. (2013) The General Structure of the Ionosphere. In: Zolesi, B. and Cander, L.R., Eds., *Ionospheric Prediction and Forecasting*, Springer Berlin Heidelberg, 11-48. https://doi.org/10.1007/978-3-642-38430-1_2

[2] Bushell, A.C. (2008) Space Weather: From Mud to Magnetopause. *Weather*, **63**, 244-245. https://doi.org/10.1002/wea.269

[3] Zawdie, K.A., Drob, D.P., Siskind, D.E. and Coker, C. (2017) Calculating the Absorption of HF Radio Waves in the Ionosphere. *Radio Science*, **52**, 767-783. https://doi.org/10.1002/2017RS006256

[4] Al'pert, Y.L. and Chang, H. (1963) Radio Wave Propagation and the Ionosphere. *Physics Today*, **16**, 69. https://doi.org/10.1063/1.3050985

[5] Davies, K. (1989) Ionospheric Radio. *IEE Electromagnetic Waves Series*, **31**, 89-152.

[6] CCIR (1982) Ionospheric Properties. In: *Propagation in Ionized Media*, *Recommendations and Reports of the CCIR*, *Rep*. 725-1, Vol. VI, International Telecommunication Union, Geneva.

[7] Chapman, S. (1931) Some Phenomena of the Upper Atmosphere. *Proceedings of the Royal Society of London*, **132**, 353-374.

[8] Wakai, N. (1971) Study on the Night-Time E Region and Its Effect on the Radio Wave Propagation. *Journal of Radio Research Laboratories* (*Japan*), **18**, 245-248.

[9] Zernov, N.N., Bisyarin, M.A. and Germ, V.E. (2023) Diffraction Theory of Propagation of High-Frequency Radio Waves in a Spherically Layered Ionospheric Radio Channel. *Journal of Communications Technology and Electronics*, **68**, 659-665. https://doi.org/10.1134/S1064226923060189

[10] Thomson, N.R., Rodger, C.J. and Clilverd, M.A. (2005) Large Solar Flares and Their Ionospheric *d* Region Enhancements. *Journal of Geophysical Research*: *Space Physics*, **110**, A06306. https://doi.org/10.1029/2005ja011008

[11] Li, W., Yue, J., Yang, Y., He, C., Hu, A. and Zhang, K. (2018) Ionospheric and Thermospheric Responses to the Recent Strong Solar Flares on 6 September 2017. *Journal of Geophysical Research*: *Space Physics*, **123**, 8865-8883. https://doi.org/10.1029/2018ja025700

[12] Curto, J.J., Marsal, S., Blanch, E. and Altadill, D. (2018) Analysis of the Solar Flare Effects of 6 September 2017 in the Ionosphere and in the Earth's Magnetic Field Using Spherical Elementary Current Systems. *Space Weather*, **16**, 1709-1720. https://doi.org/10.1029/2018sw001927

[13] Qian, L., Burns, A.G., Chamberlin, P.C. and Solomon, S.C. (2011) Variability of Thermosphere and Ionosphere Responses to Solar Flares. *Journal of Geophysical Research*: *Space Physics*, **116**, A10309. https://doi.org/10.1029/2011ja016777

[14] Sutton, J.A. (1995) The Effect of Solar and Geomagnetic Activity on Ionospheric Propagation. *IEEE Transactions on Broadcasting*, **41**, 28-34. https://doi.org/10.1109/11.372019

[15] Khoder, K., Fleury, R. and Pagani, P. (2014) Monitoring of Ionosphere Propagation Conditions Using Opportunistic HF Signals. *The* 8*th European Conference on Antennas and Propagation* (*EuCAP* 2014), The Hague, 6-11 April 2014, 2697-2701. https://doi.org/10.1109/eucap.2014.6902381

[16] ITU (n.d.) Space Services BRIFIC. http://www.itu.int/ITU-R/go/space-brific/en

[17] HF Spectrum Viewer. https://hf-spectrum.net/

[18] ITU Radiocommunication (1995) BS.705 HF Transmitting and Receiving Antennas Characteristics and Diagrams. http://www.itu.int/rec/R-REC-BS.705-1-199510-I/en

[19] Thome, G.D. and Wagner, L.S. (1971) Electron Density Enhancements in the *E* and *F* Regions of the Ionosphere during Solar Flares. *Journal of Geophysical Research*, **76**, 6883-6895. https://doi.org/10.1029/ja076i028p06883

[20] Sanon, L.W., Compaoré, W.O., Koala, S. and Zerbo, J.L. (2025) On the Occurrence of Different Classes of Solar Flares during the Solar Cycles 23 and 24. *Journal of High Energy Physics*, *Gravitation and Cosmology*, **11**, 28-38. https://doi.org/10.4236/jhepgc.2025.111004

[21] Donnelly, R.F. (1976) Empirical Models of Solar Flare X Ray and EUV Emission for Use in Studying Their *E* and *F* Region Effects. *Journal of Geophysical Research*, **81**, 4745-4753. https://doi.org/10.1029/ja081i025p04745

[22] Klobuchar, J.A. (1997) Real-Time Ionospheric Science: The New Reality. *Radio Science*, **32**, 1943-1952. https://doi.org/10.1029/97rs01234

[23] Afraimovich, E.L. (2000) GPS Global Detection of the Ionospheric Response to Solar Flares. *Radio Science*, **35**, 1417-1424. https://doi.org/10.1029/2000rs002340

[24] Zhang, D.H., Xiao, Z., Igarashi, K. and Ma, G.Y. (2002) GPS-Derived Ionospheric Total Electron Content Response to a Solar Flare That Occurred on 14 July 2000. *Radio Science*, **37**, 19-1-19-11. https://doi.org/10.1029/2001rs002542

[25] Maurya, A.K., Venkatesham, K., Kumar, S., Singh, R., Tiwari, P. and Singh, A.K. (2018) Effects of St. Patrick's Day Geomagnetic Storm of March 2015 and of June 2015 on Low-Equatorial *D* Region Ionosphere. *Journal of Geophysical Research*: *Space Physics*, **123**, 6836-6850. https://doi.org/10.1029/2018ja025536

[26] Atıcı, R. and Sağır, S. (2020) Global Investigation of the Ionospheric Irregularities during the Severe Geomagnetic Storm on September 7-8, 2017. *Geodesy and Geodynamics*, **11**, 211-221. https://doi.org/10.1016/j.geog.2019.05.004

[27] Sakurai, K. (1968) Development of Sudden Ionospheric Disturbances (SID) Associated with Solar Cosmic-Ray Flares. *Journal of Geomagnetism and Geoelectricity*, **20**,

271-280. https://doi.org/10.5636/jgg.20.271

[28] Yasyukevich, Y., Astafyeva, E., Padokhin, A., Ivanova, V., Syrovatskii, S. and Podlesnyi, A. (2018) The 6 September 2017 X-Class Solar Flares and Their Impacts on the Ionosphere, GNSS, and HF Radio Wave Propagation. *Space Weather*, **16**, 1013-1027. https://doi.org/10.1029/2018sw001932

[29] Zaalov, N.Y., Moskaleva, E.V., Rogov, D.D. and Zernov, N.N. (2015) Influence of X-Ray and Polar Cap Absorptions on Vertical and Oblique Sounding Ionograms on Different Latitudes. *Advances in Space Research*, **56**, 2527-2541. https://doi.org/10.1016/j.asr.2015.09.008

[30] Berngardt, O.I., Ruohoniemi, J.M., Nishitani, N., Shepherd, S.G., Bristow, W.A. and Miller, E.S. (2018) Attenuation of Decameter Wavelength Sky Noise during X-Ray Solar Flares in 2013-2017 Based on the Observations of Midlatitude HF Radars. *Journal of Atmospheric and Solar-Terrestrial Physics*, **173**, 1-13. https://doi.org/10.1016/j.jastp.2018.03.022

[31] Sharma, S., Chandra, H., Vats, H.O., Pandya, N.Y. and Jain, R. (2010) Ionospheric Modulations Due to Solar Flares Over Ahmadabad. *Indian Journal of Radio and Space Physics*, **39**, 296-301.

[32] NOAA SWPC: X-Ray Flux Plots. https://www.swpc.noaa.gov/products/goes-x-ray-flux

[33] Hamwaves: Ionospheric Sounding Viewer. https://hamwaves.com/ionograms/en/index.html